Biomath Communications
www.biomathforum.org/biomath/index.php/conference

A note on the n–stage growth model. Overview

Svetoslav Markov[1], Anton Iliev[2,1,3], Asen Rahnev[2], Nikolay Kyurkchiev[2,1]

[1] Institute of Mathematics & Informatics
Bulgarian Academy of Sciences
Acad. G. Bonchev Str., Bl. 8, 1113 Sofia, Bulgaria

[2] Faculty of Mathematics and Informatics
University of Plovdiv Paisii Hilendarski
24 Tzar Asen Str., 4000 Plovdiv, Bulgaria

smarkov@bio.bas.bg, aii@uni-plovdiv.bg,
assen@uni-plovdiv.bg, nkyurk@uni-plovdiv.bg

Abstract. In this paper we study the one–sided Hausdorff approximation of the generalized cut function by sigmoidal general n–stage growth model. We show that under some conditions the model is useful insofar as the theory of sigmoidal functions is well developed. The estimates of the value of the best Hausdorff approximation obtained in this article can be used in practice as one possible additional

[3]Corresponding author

Citation: Svetoslav Markov, Anton Iliev, Asen Rahnev, Nikolay Kyurkchiev, A note on the n–stage growth model. Overview, Biomath Communications 5, pp. 79-100, https://doi.org/10.11145/bmc.2018.11.117

criterions in "saturation" and "lag–time" study. As an illustrative example we consider the modelling of the growth of red abalone (*Haliotis Rufescens*) in Northern California. Numerical examples are presented using *CAS MATHEMATICA*.

Keywords: modified n–stage growth model, generalized cut function associated to the model, Hausdorff distance, upper and lower bounds

1 Introduction

Let us examine the following three–stage growth model

$$A \xrightarrow{k_1} B \xrightarrow{k_2} C \tag{1}$$

with two steps (k_1 and k_2) depending on the ratio of the growth parameters $\frac{k_1}{k_2}$.

For the mechanism the following system of ODEs is known [1]:

$$\begin{aligned} \frac{dA(t)}{dt} &= -k_1 A(t), \\ \frac{dB(t)}{dt} &= k_1 A(t) - k_2 B(t), \\ \frac{dC(t)}{dt} &= k_2 B(t), \\ A(0) &= A_0, \quad B(0) = 0, \quad C(0) = 0. \end{aligned} \tag{2}$$

Noticing that

$$\frac{dA(t)}{dt} + \frac{dB(t)}{dt} + \frac{dC(t)}{dt} = 0,$$

hence $A + B + C = A_0$, and at any time, we find

$$C(t) = A_0 - B(t) - A(t). \tag{3}$$

From the first equation of the system (2) we find

$$A(t) = A_0 e^{-k_1 t}. \tag{4}$$

The equation

$$\frac{dB(t)}{dt} + k_2 B(t) = k_1 A_0 e^{-k_1 t} \tag{5}$$

is Leibnitz's differential equation with the solution:

$$\begin{aligned} B(t) &= e^{-\int k_2\,dt} \int_0^t k_1 A_0 e^{-k_1 t} e^{\int k_2\,dt}\,dt + Re^{-\int k_2\,dt} \\ &= e^{-k_2 t} k_1 A_0 \int_0^t e^{-k_1 t} e^{k_2 t}\,dt + Re^{-k_2 t} \\ &= e^{-k_2 t} k_1 A_0 \tfrac{1}{k_2-k_1} \int_0^t de^{(k_2-k_1)t} + Re^{-k_2 t} \\ &= e^{-k_2 t} \tfrac{k_1 A_0}{k_2-k_1} \left(e^{(k_2-k_1)t} - 1\right) + Re^{-k_2 t} \\ &= \tfrac{k_1 A_0}{k_2-k_1} \left(e^{-k_1 t} - e^{-k_2 t}\right) + Re^{-k_2 t}. \end{aligned}$$

For $t = 0$ we have $B(t = 0) = 0 = R$ and

$$B(t) = \frac{k_1 A_0}{k_2 - k_1} \left(e^{-k_1 t} - e^{-k_2 t}\right). \tag{6}$$

Hence we obtain the model

$$C(t) = A_0 \left(1 - \frac{k_1}{k_2 - k_1} \left(e^{-k_1 t} - e^{-k_2 t}\right) - e^{-k_1 t}\right) \tag{7}$$

For some details, see [2], [3].

We note that the equation (6) is the general expression for the decay of a radionuclide, formed another radionuclide [2] (Chapter 5).

In [4], the authors debated to the following modified model for the individual growth of marine invertebrates:

$$\tilde{C}(t) = A_0 \left(1 - \frac{k_1}{n} \left(e^{-k_1 t} - e^{-k_2 t}\right) - e^{-k_2 t}\right)$$

where $n = k_2 - k_1$, and $\frac{k_1}{k_2}$ is close to 1.

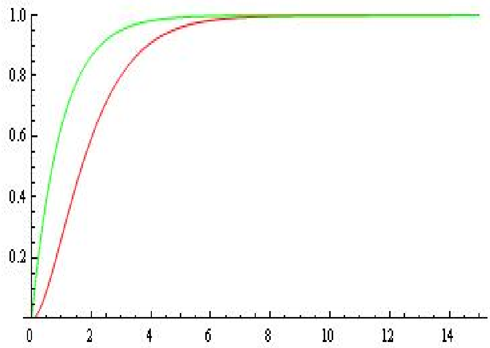

Figure 1: Three–stage growth model $\tilde{C}(t)$ (sigmoidal; red) for $n = k_2 - k_1$, $k_1 = 1$, $k_2 = 1.001$ and three–stage model $C(t)$ (first order; green) for $n = k_1 - k_2$, $k_1 = 1$, $k_2 = 2500$.

The model $\tilde{C}$ predicts sigmoidal growth (see, Fig. 1), i.e. in a three–stage growth model, the shape is controlled by the ratio $\frac{k_1}{k_2}$ [5].

For $3D$–surface plot for the three–stage mechanism in the range $n = k_2 - k_1$, or $n = k_1 - k_2$, see, Fig. 2 [5].

Without loosing of generality, for $A_0 = 1$ and $n = k_2 - k_1 > 0$, $\frac{k_1}{k_2} \to 1$ we consider the following family:

$$\tilde{C}(t) = 1 - \frac{k_1}{n}\left(e^{-k_1 t} - e^{-k_2 t}\right) - e^{-k_2 t}. \tag{8}$$

We find that the sigmoid (8) has an inflection at point:

$$t^* = \frac{1}{n}\ln\left(\frac{\left(-k_2^2 + \frac{k_1 k_2^2}{n}\right)n}{k_1^3}\right).$$

Definition 1. *The associate to the (8) cut function $\tilde{C}^*$ is defined by*

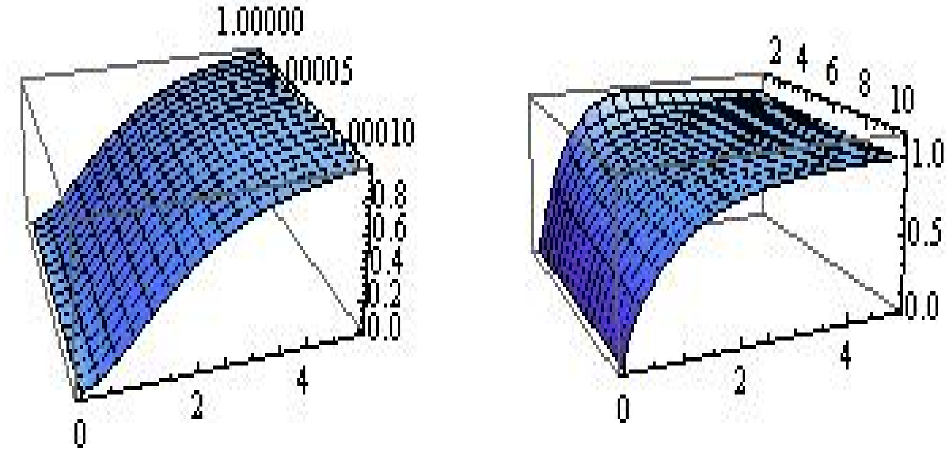

Figure 2: $3D$–surface plot for the three–stage mechanism in the range $n = k_2 - k_1$, or $n = k_1 - k_2$ [5].

[5]

$$\tilde{C}^*(t) = \begin{cases} 0, & if \quad t < t_1, \\ \tilde{C}'(t^*)(t - t^*) + \tilde{C}(t^*), & if \quad t_1 \le t < t_2, \\ 1, & if \quad t \ge t_2. \end{cases} \tag{9}$$

The straight line $y = \tilde{C}'(t^*)(t - t^*) + \tilde{C}(t^*)$ crosses the lines $y = 0$ and $y = 1$ at the points t_1 and t_2.

Definition 2. *[6] The one–sided Hausdorff distance $\overrightarrow{\rho}(f, g)$ between two interval functions f, g on $\Omega \subseteq \mathbb{R}$, is the one–sided Hausdorff distance between their completed graphs $\mathcal{F}(f)$ and $\mathcal{F}(g)$ considered as closed subsets of $\Omega \times \mathbb{R}$. More precisely,*

$$\overrightarrow{\rho}(f, g) = \sup_{B \in \mathcal{F}(g)} \inf_{A \in \mathcal{F}(f)} ||A - B||,$$

where $|| \cdot ||$ is a norm in $\mathbb{R}^2$.

We recall that completed graph of f is the closure of the graph of f as a subset of $\Omega \times \mathbb{R}$. If the graph of an interval function f equals $\mathcal{F}(f)$, then the f is called S-continuous.

The Hausdorff distance $\rho(f,g) = \max\{\overrightarrow{\rho}(f,g), \overrightarrow{\rho}(g,f)\}$ defines a metric in the set of the S-continuous interval functions [7]–[10].

The one–sided Hausdorff distance d between the functions (8) and (9) satisfies the relation

$$\tilde{C}(t_2 + d) = 1 - d. \tag{10}$$

The following theorem gives upper and lower bounds for d

Theorem A [5]. *Let*

$$p = -e^{-k_2 t_2} - \frac{k_1}{n} e^{-k_1 t_2} + \frac{k_1}{n} e^{-k_2 t_2},$$

$$q = 1 + k_2 e^{-k_2 t_2} + \frac{k_1^2}{n} e^{-k_1 t_2} - \frac{k_1 k_2}{n} e^{-k_2 t_2},$$

$$r = -2\frac{q}{p};\ \ n = k_2 - k_1 > 0;\ \ \frac{k_1}{k_2} \to 1;\ \ \frac{2k_1 - k_2}{k_1} < e^{t_2(k_2 - k_1)}.$$

For the one–sided Hausdorff distance d between $\tilde{C}^*(t)$ and the sigmoidal function (8) the following inequalities hold for: $r > e^2$

$$d_l = \frac{1}{r} < d < \frac{\ln r}{r} = d_r. \tag{11}$$

The model (8) for $k_1 = 1$, $k_2 = 1.01$, $t^* = 0.985033$, $t_1 = 0.27045$, $t_2 = 2.97525$ is visualized on Fig. 3.

From the nonlinear equation (10) and inequalities (11) we have: $d = 0.174444$, $d_l = 0.0865764$, $d_r = 0.211829$.

The estimates of the value of the best Hausdorff approximation can be used in practice as one possible additional criterion in "saturation" study.

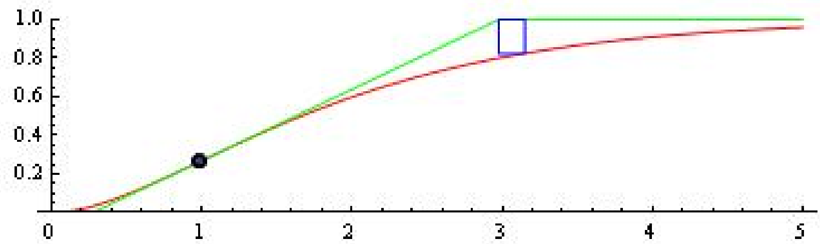

Figure 3: The cut function $\tilde{C}^*(t)$ and the sigmoidal function $\tilde{C}(t)$ with $k_1 = 1$, $k_2 = 1.01$, $t^* = 0.985033$, $t_1 = 0.27045$, $t_2 = 2.97525$; H–distance $d = 0.174444$, $d_l = 0.0865764$, $d_r = 0.211829$.

2 Main Results

2.1 The four–stage growth model

Let us examine the following four–stage growth model

$$A \xrightarrow{k_1} B \xrightarrow{k_2} C \xrightarrow{k_3} D \tag{12}$$

For the mechanism the following system of ODEs is known:

$$\begin{aligned}
\frac{dA(t)}{dt} &= -k_1 A(t),\\
\frac{dB(t)}{dt} &= k_1 A(t) - k_2 B(t),\\
\frac{dC(t)}{dt} &= k_2 B(t) - k_3 C(t),\\
\frac{dD(t)}{dt} &= k_3 C(t),\\
A(0) &= A_0, \quad B(0) = 0, \quad C(0) = 0, \quad D(0) = 0.
\end{aligned} \tag{13}$$

Noticing that

$$\frac{dA(t)}{dt} + \frac{dB(t)}{dt} + \frac{dC(t)}{dt} + \frac{dD(t)}{dt} = 0,$$

hence $A + B + C + D = A_0$, and at any time, we find

$$D(t) = A_0 - C(t) - B(t) - A(t). \tag{14}$$

Calculate $C(t)$, assuming that $C(0) = 0$

$$\begin{aligned}
C(t) =&\ e^{-\int k_3\,dt} \int_0^t \tfrac{k_1k_2A_0}{k_2-k_1} \left(e^{-k_1t} - e^{-k_2t}\right) e^{\int k_3\,dt}\,dt \\
=&\ e^{-k_3t} \tfrac{k_1k_2A_0}{k_2-k_1} \int_0^t \left(e^{-k_1t} - e^{-k_2t}\right) e^{k_3t}\,dt \\
=&\ e^{-k_3t} \tfrac{k_1k_2A_0}{k_2-k_1} \left(\int_0^t e^{(k_3-k_1)t}\,dt - \int_0^t e^{(k_3-k_2)t}\,dt\right) \\
=&\ e^{-k_3t} \tfrac{k_1k_2A_0}{k_2-k_1} \left(\tfrac{1}{k_3-k_1} \int_0^t\, de^{(k_3-k_1)t} - \tfrac{1}{k_3-k_2} \int_0^t\, de^{(k_3-k_2)t}\right) \\
=&\ e^{-k_3t} \tfrac{k_1k_2A_0}{k_2-k_1} \left(\tfrac{e^{(k_3-k_1)t}}{k_3-k_1} - \tfrac{1}{k_3-k_1} - \tfrac{e^{(k_3-k_2)t}}{k_3-k_2} + \tfrac{1}{k_3-k_2}\right) \\
=&\ k_1k_2A_0 \left(\tfrac{e^{-k_1t}}{(k_2-k_1)(k_3-k_1)} + \tfrac{e^{-k_2t}}{(k_1-k_2)(k_3-k_2)} + \tfrac{e^{-k_3t}}{(k_1-k_3)(k_2-k_3)}\right).
\end{aligned} \tag{15}$$

From (4), (6) and (15) we find

$$\begin{aligned}
D(t) =&\ A_0 \Big(1 - \tfrac{k_1}{k_2-k_1} \left(e^{-k_1t} - e^{-k_2t}\right) - \\
&\quad k_1k_2 \left(\tfrac{e^{-k_1t}}{(k_2-k_1)(k_3-k_1)} + \tfrac{e^{-k_2t}}{(k_1-k_2)(k_3-k_2)} + \tfrac{e^{-k_3t}}{(k_1-k_3)(k_2-k_3)}\right) - e^{-k_1t}\Big).
\end{aligned} \tag{16}$$

Without loosing of generality, for $A_0 = 1$ and $k_3 > k_2 > k_1 > 0$, $\frac{k_3}{k_1} \to 1$, $\frac{k_3}{k_2} \to 1$ we consider the following family:

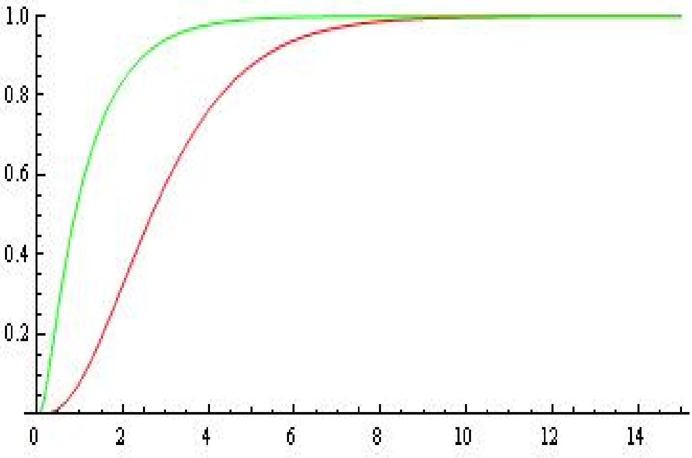

Figure 4: Four–stage growth model $\tilde{D}(t)$ (sigmoidal; red) for $k_1 = 1$, $k_2 = 1.001$, $k_3 = 1.002$ and $\tilde{D}(t)$ (first order; green) for $k_1 = 1$, $k_2 = 10$, $k_3 = 12$.

$$\begin{aligned}\tilde{D}(t) &= 1 - \tfrac{k_1}{k_2-k_1}\left(e^{-k_1 t} - e^{-k_2 t}\right) - \\ &\qquad k_1 k_2 \left(\tfrac{e^{-k_1 t}}{(k_2-k_1)(k_3-k_1)} + \tfrac{e^{-k_2 t}}{(k_1-k_2)(k_3-k_2)} + \tfrac{e^{-k_3 t}}{(k_1-k_3)(k_2-k_3)}\right) - e^{-k_1 t}.\end{aligned} \tag{17}$$

The model $\tilde{D}$ predicts sigmoidal growth (see, Fig. 4), i.e. in a four–stage growth model, the shape is controlled by the ratio $\frac{k_3}{k_1}$ and ratio $\frac{k_3}{k_2}$.

Let the sigmoid (17) has an inflection point t^*.

Consider the following associate to the (17) cut function $\tilde{D}^*$

$$\tilde{D}^*(t) = \begin{cases} 0, & if \quad t < t_1, \\ \tilde{D}'(t^*)(t-t^*) + \tilde{D}(t^*), & if \quad t_1 \le t < t_2, \\ 1, & if \quad t \ge t_2. \end{cases} \tag{18}$$

The straight line $y = \tilde{D}'(t^*)(t-t^*) + \tilde{D}(t^*)$ crosses the lines $y = 0$ and $y = 1$ at the points t_1 and t_2.

The one–sided Hausdorff distance d between the functions (17) and (18) satisfies the relation

$$\tilde{D}(t_2 + d) = 1 - d. \tag{19}$$

The following theorem gives upper and lower bounds for d

Theorem B. Let

$$\begin{aligned} p &= -e^{-k_1 t_2} - \tfrac{k_1}{k_2-k_1}\left(e^{-k_1 t_2} - e^{-k_2 t_2}\right) - \\ &\quad k_1 k_2 \left(\tfrac{e^{-k_1 t_2}}{(k_2-k_1)(k_3-k_1)} + \tfrac{e^{-k_2 t_2}}{(k_1-k_2)(k_3-k_2)} + \tfrac{e^{-k_3 t_2}}{(k_1-k_3)(k_2-k_3)}\right), \\ q &= 1 + e^{-k_1 t_2} k_1 + \tfrac{k_1^2}{k_2-k_1} e^{-k_1 t_2} - \tfrac{k_1 k_2}{k_2-k_1} e^{-k_2 t_2} + \\ &\quad k_1 k_2 \left(\tfrac{e^{-k_1 t_2} k_1}{(k_2-k_1)(k_3-k_1)} + \tfrac{e^{-k_2 t_2} k_2}{(k_1-k_2)(k_3-k_2)} + \tfrac{e^{-k_3 t_2} k_3}{(k_1-k_3)(k_2-k_3)}\right), \\ r &= -2\tfrac{q}{p}; \;\; k_3 > k_2 > k_1 > 0, \;\; \tfrac{k_3}{k_1} \to 1, \;\; \tfrac{k_3}{k_2} \to 1. \end{aligned} \tag{20}$$

For the one–sided Hausdorff distance d between $\tilde{D}^*(t)$ and the sigmoidal function (17) the following inequalities hold for: $r > e^2$

$$d_l = \frac{1}{r} < d < \frac{\ln r}{r} = d_r. \tag{21}$$

Proof. Let us examine the function:

$$F(d) = \tilde{D}(t_2 + d) - 1 + d. \tag{22}$$

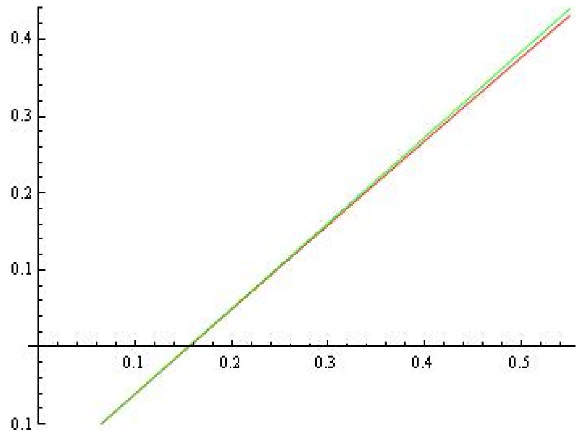

Figure 5: The functions $F(d)$ and $G(d)$ for $k_1 = 1; k_2 = 1.001; k_3 = 1.002$.

From $F'(d) > 0$ we conclude that function F is increasing.

Consider the function

$$G(d) = p + qd. \tag{23}$$

From Taylor expansion we obtain $G(d) - F(d) = O(d^2)$.

Hence $G(d)$ approximates $F(d)$ with $d \to 0$ as $O(d^2)$ (see Fig. 5). In addition $G'(d) > 0$.

From the conditions of the theorem, we see that $p < 0$ and $q > 0$ (for some details, see [5]) and $G(d_l) < 0$, $G(d_r) > 0$.

This completes the proof of the theorem.

The model (17) for $k_1 = 1$, $k_2 = 1.001$, $k_3 = 1.002$, $t^* = 1.998$, $t_1 = 0.80467$, $t_2 = 4.4955$ is visualized on Fig. 5.

From the nonlinear equation (19) and inequalities (21) we have: $d = 0.15669$, $d_l = 0.0772965$, $d_r = 0.197887$.

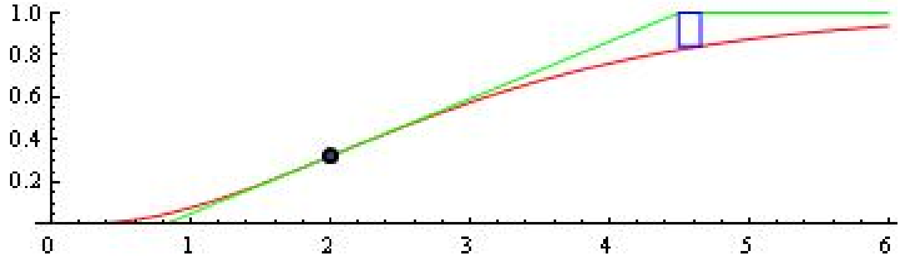

Figure 6: The cut function $\tilde{D}^*(t)$ and the sigmoidal function $\tilde{D}(t)$ with $k_1 = 1$, $k_2 = 1.001$, $k_3 = 1.002$, $t^* = 1.998$, $t_1 = 0.80467$, $t_2 = 4.4955$; H– distance $d = 0.15669$, $d_l = 0.0772965$, $d_r = 0.197887$.

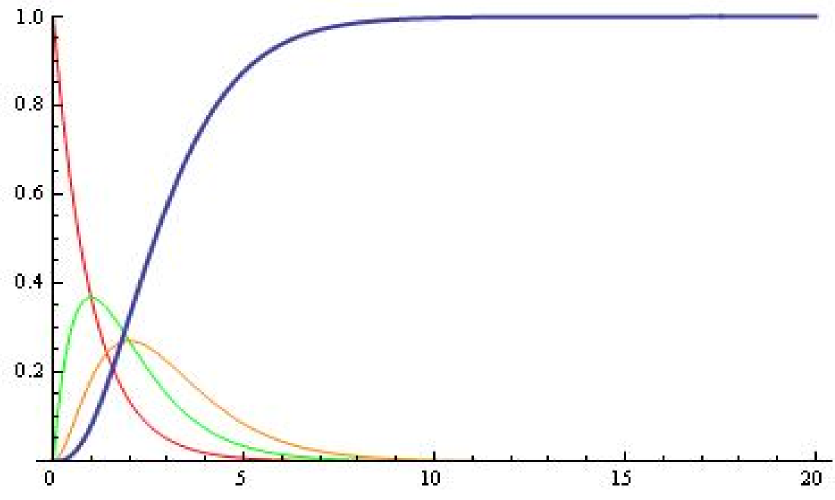

Figure 7: The solution of the system of ODEs (13): $A(t)$ (red), $B(t)$ (green), $C(t)$ (orange) and $D(t)$ (sigmoid; thick) for $k_1 = 1$, $k_2 = 1.001$, $k_3 = 1.002$.

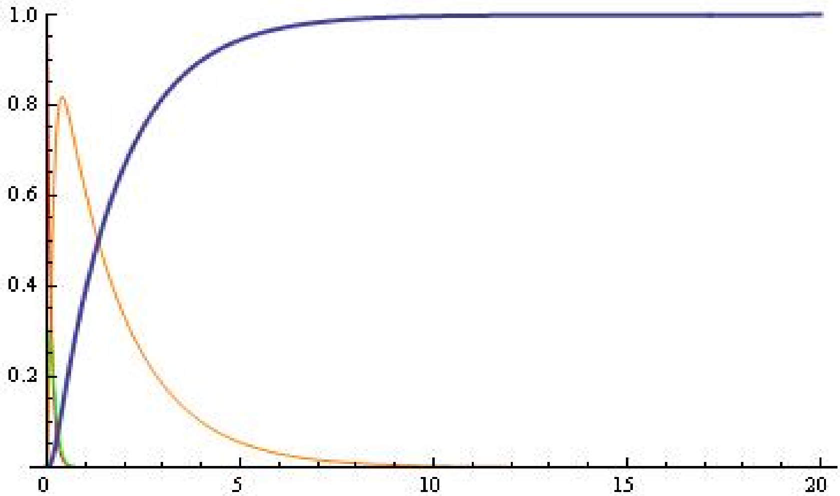

Figure 8: The solution of the system of ODEs (13): $A(t)$ (red), $B(t)$ (green), $C(t)$ (orange) and $D(t)$ (first order; inflection point $t^* = 1.00592 \times 10^{-16} \approx 0$; thick) for $k_1 = 10$, $k_2 = 15$, $k_3 = 0.6$.

The solution of the system of ODEs (13) with $k_1 = 1$, $k_2 = 1.001$, $k_3 = 1.002$ and $A(0) = 1$, $B(0) = 0$, $C(0) = 0$, $D(0) = 0$ is plotted on Fig. 7.

In a strongly disturbed order of the reaction constants k_i, for example $k_1 = 10$, $k_2 = 15$, $k_3 = 0.6$, the solution of the ODEs is depicted in Fig. 8.

Growth curves are found in a wide range of disciplines, such as biology, chemistry and medical science.

Estimating the lag time in the growth process is a practically important problem, as it may indicate a successful therapy for a number of diseases.

The curve $\tilde{C}(t)$ is typically divided into the lag phase, the growth phase, and the plateau phase.

The inflection time t^* is when the growth rate reaches its maximum. The lag time is then typically estimated by extending the tangent at

t^* down to the time axis.

Nevertheless, any sigmoid function can be good illustration for the concept of lag time [11].

2.2 The general case

Let us examine the general case

$$N_1 \xrightarrow{k_1} N_2 \xrightarrow{k_2} N_3 \xrightarrow{k_3} \cdots N_{n-1} \xrightarrow{k_{n-1}} N_n, \tag{24}$$

For the mechanism the following system of ODEs is known:

$$\begin{aligned}
\frac{dN_1(t)}{dt} &= -k_1 N_1(t), \\
\frac{dN_2(t)}{dt} &= k_1 N_1(t) - k_2 N_2(t), \\
\cdots & \\
\frac{dN_{n-1}(t)}{dt} &= k_{n-2} N_{n-2}(t) - k_{n-1} N_{n-1}(t), \\
\frac{dN_n(t)}{dt} &= k_{n-1} N_{n-1}(t).
\end{aligned} \tag{25}$$

Let $N_1(0) = A_0 = 1;\ N_2(0) = \cdots = N_{n-1}(0) = N_n(0) = 0$.

Noticing that

$$\frac{dN_1(t)}{dt} + \frac{dN_2(t)}{dt} + \cdots + \frac{dN_{n-1}(t)}{dt} + \frac{dN_n(t)}{dt} = 0,$$

hence $N_1 + N_2 + \cdots + N_{n-1} + N_n = A_0 = 1$, and at any time, we find

$$N_n(t) = 1 - \sum_{i=1}^{n-1} N_i(t)$$

or

$$N_n(t) = 1 - \sum_{i=2}^{n-1} N_i(t) - e^{-k_1 t}. \tag{26}$$

The solutions $N_i(t)$; $i = 2, 3, \ldots, n-1$ can be generated by the formula of Bateman [3]:

$$N_l(t) = k_1 k_2 \ldots k_{l-1} \sum_{i=1}^{l} W_i e^{-k_i t}; \quad l = 2, 3, \ldots, n-1 \qquad (27)$$

where

$$W_i = \prod_{\substack{j = 1 \\ i \neq i}}^{l} \frac{1}{k_j - k_i}.$$

3 Numerical example.

We examine the following data. (The small data for modeling the growth of red abalone is shown in Table 1. For more details, see [12]).

The model $\tilde{D}(t)$ (17) based on the data of Table 1 for the estimated parameters:

$$A_0 = 179.6; \;\; k_1 = 0.575; \;\; k_2 = 0.58; \;\; k_3 = 0.593622$$

is plotted on Fig. 9.

4 Concluding Remarks

.

The model (26) has a certain right of existence insofar as the theory of sigmoidal functions is well developed.

The estimates of the value of the best Hausdorff approximation obtained in this article can be used in practice as one possible additional criterion in "saturation" study.

Age	$Length(mm)$
1	16.1
2	33.9
3	54.3
4	76.2
5	97.8
6	117.1
7	133.3
8	146.5
9	157.2
10	166
11	173.3
12	179.6

Table 1: Data for modeling the growth of red abalone *Haliotis Rufescens* in Northern California [12]

For some approximation, computational and modelling aspects, see [13]–[40].

The results obtained in this paper can be used when controlling growth in Software Reliability Models, see [41]–[44].

Based on the methodology proposed in the present note, the reader may formulate the corresponding approximation problems for the general model $N_n(t)$ (26) on his/her own.

Acknowledgment

This work has been supported by the project BG05M2OP001-1.001-0003-01 "CoE on Informatics and ICT" supported by the Operational Programme "Science and Education for Smart Growth".

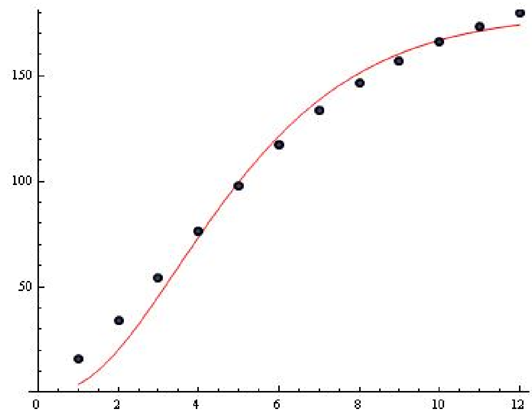

Figure 9: The model $\tilde{D}(t)$

References

[1] A. Cornish–Bowden, Fundamentals of Enzyme Kinetics, Wiley–Blackwell, 2012, ISBN: 978-3-527-33074-4.

[2] D. Soete, R. Gijbels, J. Hoste, Neuron Activation Analysis, Wiley–Interscience, 1972.

[3] H. Bateman, The solution of a system of differential equations occurring in the theory of radio–active transformations, Proc. Cambridge Phil. Soc., **15** 1910, 423–427.

[4] L. Rogers–Bennett, D. W. Rogers, A two–step growth curve: Approach to the von Bertalanffy and Gompertz equations, Adv. in Pure Math., **6** 2016, 321–330.

[5] S. Markov, A. Iliev, A. Rahnev, N. Kyurkchiev, A note on the three–stage growth model, Dynamic Systems and Applications, **28**(1) 2019, 63–72.

[6] B. Sendov, Hausdorff Approximations, Kluwer, Boston, 1990.

[7] R. Anguelov, S. Markov, Hausdorff Continuous Interval Functions and Approximations, In: SCAN 2014 Proceedings, LNCS, ed. by J.W.von Gudenberg, Springer, Berlin, 2015.

[8] R. Anguelov, S. Markov, B. Sendov, On the Normed Linear Space of Hausdorff Continuous Functions. In: Lirkov, I., et al. (Eds.): Lecture Notes in Computer Science, **3743**, Springer, 2006, 281–288.

[9] R. Anguelov, S. Markov, B. Sendov, Algebraic Operations on the Space of Hausdorff Continuous Functions. In: Bojanov, B. (Ed.): Constructive Theory of Functions, Prof. M. Drinov Academic Publ. House, Sofia, 2006, 35–44.

[10] R. Anguelov, S. Markov, B. Sendov, The Set of Hausdorff Continuous Functions - the Largest Linear Space of Interval Functions, Reliable Computing, **12** 2006, 337–363.

[11] S. Shoffner, S. Schnell, Estimation of the lag time in a subsequent monomer addition model for fibrill elongation, bioRxiv The preprint server for biology, doi:10.1101/034900, 2015, 1–8.

[12] L. Rogers–Bennett, D. W. Rogers, S. A. Schultz, Modeling growth and mortality of red abalone *Haliotis Rufescens* in Northern California, J. of Shellfish Research, **26**(3) 2007, 719–727.

[13] N. Kyurkchiev, S. Markov, On the Hausdorff distance between the Heaviside step function and Verhulst logistic function, J. Math. Chem., **54**(1) 2016, 109–119.

[14] N. Kyurkchiev, S. Markov, Sigmoid functions: Some Approximation and Modelling Aspects, LAP LAMBERT Academic Publishing, Saarbrucken, 2015, ISBN 978-3-659-76045-7.

[15] N. Kyurkchiev, A. Iliev, S. Markov, Some Techniques for Recurrence Generating of Activation Functions: Some Modeling and Approximation Aspects, LAP LAMBERT Academic Publishing, 2017, ISBN: 978-3-330-33143-3.

[16] R. Anguelov, M. Borisov, A. Iliev, N. Kyurkchiev, S. Markov, On the chemical meaning of some growth models possessing Gompertzian-type property, Math. Meth. Appl. Sci., 2017, 1–12, doi:10.1002/mma.4539.

[17] R. Anguelov, N. Kyurkchiev, S. Markov, Some properties of the Blumberg's hyper-log-logistic curve, BIOMATH, **7**(1) 2018, 8 pp.

[18] A. Iliev, N. Kyurkchiev, S. Markov, On the Approximation of the step function by some sigmoid functions, Mathematics and Computers in Simulation, **133** 2017, 223–234.

[19] A. Iliev, N. Kyurkchiev, S. Markov, Approximation of the cut function by Stannard and Richards sigmoid functions, IJPAM, **109**(1) 2016, 119–128.

[20] S. Markov, A. Iliev, A. Rahnev, N. Kyurkchiev, A note on the Log-logistic and transmuted Log-logistic models. Some applications, Dynamic Systems and Applications, **27**(3) 2018, 593–607.

[21] S. Markov, N. Kyurkchiev, A. Iliev, A. Rahnev, On the approximation of the cut functions by hyper-log-logistic function, Neural, Parallel and Scientific Computations, **26**(2) 2018, 169–182.

[22] N. Kyurkchiev, A. Iliev, S. Markov, Families of recurrence generated three and four parametric activation functions, Int. J. Sci. Res. and Development, **4**(12) 2017, 746–750.

[23] N. Kyurkchiev, A note on the new geometric representation for the parameters in the fibril elongation process, C. R. Acad. Bulg. Sci., **69**(8) 2016, 963–972.

[24] N. Kyurkchiev, On the numerical solution of the general "ligand-gated neuroreceptors model' via CAS Mathematica, Pliska Stud. Math. Bulgar., **26** 2016, 133–142.

[25] N. Kyurkchiev, S. Markov, On the numerical solution of the general kinetic "K-angle" reaction system, Journal of Mathematical Chemistry, **54**(3) 2016, 792–805.

[26] L. Rogers–Bennett, D. Rogers, W. Bennett, T. Ebert, Modeling Red Sea Urchin Growth Using Six Growth Models, Fishery Bulletin, **101** 2003, 614–626.

[27] R. Leaf, L. Rogers–Bennett, Y. Jiao, Exploring the Use of a Size Based Egg per Recruit Model for the Red Abalone Fishery in California, North American Journal of Fisheries Management, **28** 2008, 1638–1647.

[28] N. Lester, B. Shuter, P. Abrams, Interpreting the von Bertalanffy Model of Somatic Growth in Fishes: The Cost of Reproduction, Proceedings of the Royal Society B: Biological Sciences, **271** 2004, 1625–1631.

[29] A. Hernandez–Llamas, D. Ratkowsky, Growth of Fishes, Crustaceans and Mollusks: Estimation of the von Bertalanffy, Logistic, Gompertz and Richards Curves and a New Growth Model, Marine Ecology Progress Series, **282** 2004, 237–244.

[30] L. von Bertalanffy, A Quantitative Theory of Organic Growth (Inquiries on Growth Laws. II), Human Biology, **10** 1938, 181–213.

[31] K. Sainsbury, Effect of Individual Variability on the von Bertalanffy Growth Equation, Canadian Journal of Fisheries and Aquatic Sciences, **37** 1980, 241–247.

[32] P. Haaker, D. Parker, K. Barsky, C. Chun, Growth of Red Abalone, Haliotis rufescens (Swainson), at Johnson's Lee Santa Rosa Island, California, Journal of Shellfish Research, **17** 1998, 747–753.

[33] N. Kyurkchiev, A. Iliev, Extension of Gompertz-type Equation in Modern Science: 240 Anniversary of the birth of B. Gompertz, LAP LAMBERT Academic Publishing, 2018, ISBN: 978-613-9-90569-0.

[34] S. Markov, N. Kyurkchiev, A. Iliev, A. Rahnev, On the approximation of the generalized cut functions of degree $p+1$ by smooth hyper-log-logistic function, Dynamic Systems and Applications, **27**(4) 2018, 715–728.

[35] O. Rahneva, H. Kiskinov, I. Dimitrov, V. Matanski, Application of a Weibull Cumulative Distribution Function Based on m Existing Ones to Population Dynamics, International Electronic Journal of Pure and Applied Mathematics, **12**(1) 2018, 111–121.

[36] J. Toth, A. L. Nagy, D. Papp, Past, Present, and Future Programs for Reaction Kinetics. In: Reaction Kinetics: Exercises, Programs and Theorems, Springer, New York, 2018, ISBN: 978-1-4939-8641-5.

[37] Y. Prostov, Y. Tiumentsev, Recurrent neurodynamic model of neuron with variable activation characteristic, Biologically Inspired Cognitive Architectures, 2018, 8 pp.

[38] N. Guliyev, V. Ismailov, On the approximation by single hidden layer feedforward neural networks with fixed weights, Neural Networks, **98** 2018, 296–304.

[39] D. Costarelli, R. Spigler, Solving numerically nonlinear systems of balance laws by multivariate sigmoidal functions approximation, Computational and Applied Mathematics, 2016, doi:10.1007/s40314-016-0334-8.

[40] D. Costarelli, R. Spigler, G. Vinti, A survey on approximation by means of neural network operators, Journal of NeuroTechnology, **1**(1) 2016, 1–24.

[41] N. Pavlov, A. Iliev, A. Rahnev, N. Kyurkchiev, Some software reliability models: Approximation and modeling aspects, LAP LAMBERT Academic Publishing, 2018, ISBN: 978-613-9-82805-0.

[42] N. Pavlov, A. Iliev, A. Rahnev, N. Kyurkchiev, Nontrivial Models in Debugging Theory (Part 2), LAP LAMBERT Academic Publishing, 2018, ISBN: 978-613-9-87794-2.

[43] V. Kyurkchiev, A. Malinova, O. Rahneva, P. Kyurkchiev, On the Burr XII-Weibull Software Reliability Model, Int. J. of Pure and Appl. Math., **119**(4) 2018, 639–650.

[44] V. Kyurkchiev, H. Kiskinov, O. Rahneva, G. Spasov, A Note on the Exponentiated Exponential-Poisson Software Reliability Model, Neural, Parallel, and Scientific Computations, **26**(3) 2018, 257–267.